Available online at www.sciencedirect.com
ScienceDirect
Chinese Journal of Aeronautics 22(2009) 121-128
Chinese Journal of Aeronautics
www.elsevier.com/locate/cja

Enhancing Aerodynamic Performances of Highly Loaded Compressor Cascades via Air Injection

Feng Dongmin, Chen Fu*, Song Yanping, Chen Huanlong, Wang Zhongqi

School of Energy Science and Engineering, Harbin Institute of Technology, Harbin 150001, China

Received 25 January 2008; accepted 14 March 2008

Abstract

This article experimentally studies the effects of air injection near the blade trailing edge on flow separation and losses in a highly loaded linear compressor cascade. Aerodynamic parameters of eight cascades with different air injection slot configurations are measured by using a five-hole probe at the cascade outlets. Ink-trace flow visualization is performed to obtain the flow details around the air injection slots. The static pressure distribution is clarified with pressure taps on the endwalls. The results indicate that air injection has little effect on the static pressure distribution on the endwalls, but improves the flow behavior at the corners between the suction surfaces and the endwalls with the decrease in losses at midspan. Slot positions have great effect on the compressor cascade performances. The optimal slot location is 25% of the blade span. The energy loss coefficient is reduced by 5.5% at most.

Keywords: highly loaded compressor; experimental study; air injection; aerodynamic performance

1. Introduction

As flow separation generally leads to increased energy losses and operating instability, its control is required to improve aerodynamic performance. Many flow separation control methods have been introduced in the published works. Recently, M. Gad-el-Hak[1] and D. Greenblatt, et al.[2] made reviews on this subject. Generally, flow control methods are classified as active and passive depending on whether some additional energy is involved.

Injection or blowing is an effective method to control the flow separation. The basic principle is to energize the decelerated fluid near the solid surface with streams of high-momentum fluid. J. P. Bons, et al.[3] and R. J. Volino[4] described the use of vortex generator jets (VGJs) to control flow separation. As an another effective way, synthetic jet is capable of re-energizing flows by delaying separation, changing effective cambers of airfoils and manipulating vortex flows[5]. A. M. Honohan, et al.[6] investigated the effects of using synthetic jets for aerodynamic control. They found that accelerating the cross flow with synthetic jets resulted in a thinner boundary layer capable of overcoming stronger adverse pressure gradients, and ultimately delaying or suppressing flow separation. X. Q. Zheng, et al.[7] showed that the periodic suction and blowing could control the disordered unsteady separate flows in a wide range of incidence and also improve the time-averaged aerodynamic performances of the axial compressor cascades.

From the above-mentioned published works, it is realized that effective for aerodynamic control, it is an active type involving use of extra energy adding complexity, and weight of the system. In contrary, passive methods are always preferable because of their simplicity and cost effectiveness. In this area, Y. P. Song, et al.[8] applied air injection to control flow separation in highly loaded compressor cascades with straight blades and compound lean blades. Of them, the computational fluid dynamics (CFD) results show that the slot configuration produces the most favorable influence on through-flow capacity enhancement and total loss reduction.

This article focuses on the experimental study on the passive control method to inject air to highly loaded compressor cascades. The air injection acts as a jet flow within the corner region near the trailing edge

*Corresponding author. Tel.: +86-451-86412368.
E-mail address: chenfu@hit.edu.cn
Foundation items: National Natural Science Foundation of China (50876023); Chinese Specialized Research Fund for the Doctoral Program of Higher Education (20060213007); National Basic Research Program of China (2007CB210100)

doi: 10.1016/S1000-9361(08)60077-1

resulted from the pressure difference between the pressure side (PS) and suction side (SS). Therefore, it is expected to energize the low energy fluid within the corner region and reduce the losses. The injected mass flow rate depends on the pressure difference between the two sides of the blade. The aim of the present study is to explore the effects of air injection on the aerodynamic performances of highly loaded compressor cascades. Particular attention is paid to the understanding of the relationship between the spanwise slot positions and the aerodynamic performances of the cascades. The Reynolds number based on the chord length and the inlet velocity is 610 000. Eight different injection slot configurations are chosen with slots located at 5%-25% of the blade height.

2. Experimental Setup

2.1. Low-speed cascade wind tunnel

The experiments were carried out in a large-scale open-circuit low-speed blower-type wind tunnel at the Engine Aerodynamic Research Center, Harbin Institute of Technology. In this tunnel, air was filtered before entering a centrifugal blower, where the pressure was to be increased. The air then passed a honeycomb and a series of screens to prevent swirl and turbulence. Next, the flow was accelerated through a three-dimensional contraction nozzle before entering the test section. In this study, the inlet boundary layer thickness was measured to be about 10 mm. The low-speed wind tunnel permits testing cascades at low speeds with the maximum attainable $Ma = 0.3$. The five-hole probe used in the experiments was calibrated separately in a low-speed calibration tunnel at direction-sensitive lower velocities, which was of ±30° yaw and ±30° pitch to give a calibration map made up of 29° yaw angles and 29° pitch angles. Pressure transducers of PM10-1-2-S-0 type with a rated range of 0-1 000 mmH_2O (1 mmH_2O = 9.806 65 Pa) were used to measure the pressures stored in a computer. At each measurement point, the data collection took 3 s, during which approximately 500-1 500 pressure values were registered and averaged to eliminate the effects of airflow fluctuation. The displacement error of the probe was taken to be 0.5 mm in the spanwise direction and less than 1° in the pitch-wise direction. The static pressure distribution on the endwall was measured by a pilot pressure gauge with the accuracy of 0.5 mmH_2O. The uncertainty of the energy loss coefficients was assumed to be approximately 0.04. More detailed discussion about the accuracy of measurements by the presented methods is given in Ref.[9].

The inlet and outlet aerodynamic parameters measured in the experiments include local velocities, pressures and static pressure distribution on surfaces. Fig.1 shows the measurement locations of static pressure on the endwall. The flow field downstream of the cascade is measured at 46.7% of the axial chord downstream of the trailing edge. The traversing plane is shifted relative to the wake centerlines to capture the entire wake and the loss core downstream of a blade. All the measurements are conducted on the lower half of the blade because both halves of a linear compressor cascade are symmetrical with respect to the midspan. The NACA65 profile with 60º camber angles is selected to attain a large diffusion within the stator passage. The geometrical and aerodynamic parameters of the cascade and the injection slot are as follows: chord length $b = 128$ mm; axial blade chord $B = 122$ mm; blade height $H = 160$ mm; aspect ratio $A_r = 1.25$; pitch $t = 94$ mm; inlet metal angle $\beta_{1P} = 48.2°$; outlet metal angle $\beta_{2P} = -11.8°$; stagger angle $\beta_b = 18.2°$; slot height $D = 3.5$ mm; slot spanwise location $H_s = 8$, 24, 40 mm. Fig.2 describes the slot configuration. All measurements are carried out at the design incidence.

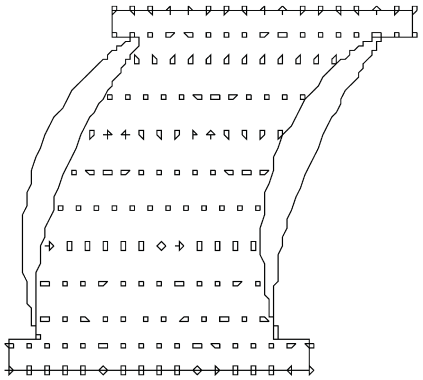

Fig.1 Distribution of static pressure taps on endwall.

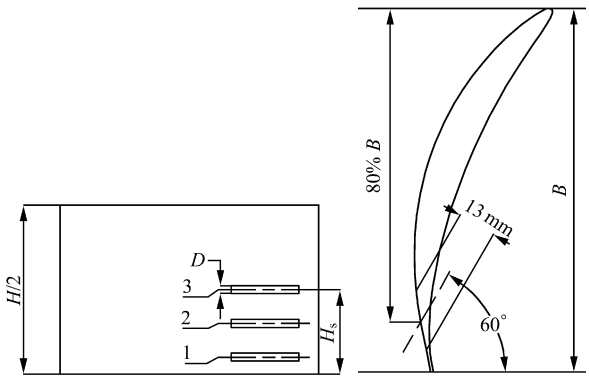

Fig.2 Definition of slot configurations.

2.2. Air injection implementation

Air injection configurations are used in the present study to control boundary layer losses under highly loaded compressor conditions. The determination of the optimum injection slot configuration in terms of slot spanwise location and slot orientation (yaw angle) is carried out in the linear compressor cascade. Fig.2 illustrates the three spanwise locations of a one slot configuration, marked by 1, 2, and 3, respectively.

Eight configurations were tested in the experiments designated by:

(1) D0—the baseline configuration without a slot in the blade.

(2) D1, D2, and D3—single slot configurations characterized by H_s/H equal to 0.05, 0.15, and 0.25, respectively. Further, the configuration D1 had the slot 1 spanwise at 0.05 of the blade height; D2 the slot 2 at 0.15; and D3 the slot 3 at 0.25.

(3) D4, D5, and D6—the double slot configurations with D4 being the combination of D1 and D2, D5 of D1 and D3, and D6 of D2 and D3.

(4) D7—the triple slot configuration, in which slots 1, 2, and 3 were used simultaneously for air injection.

3. Results and Discussion

Fig.3 shows the contours of the static pressure coefficients on the cascade endwall. The static pressure coefficient (C_p) is defined as

$$C_p = p_s/(p_1^* - p_1) \tag{1}$$

where p_s is local static pressure, p_1 inlet static pressure and p_1^* inlet total pressure.

For simplicity, only static pressure distribution of D0 and D1 are presented in Fig.3, because D2, D3, and D6 have the distribution similar to D0, and D4, D5, and D7 to D1. Compared with D0, the area between the contour lines of –0.10 and –0.15 near the suction surface and the trailing edge enlarges. This means that the static pressure increases in this region. Near the pressure surface, the static pressure in terms of the static pressure coefficient reduces from 0.25 to 0.20 because of the injection slot at 5% of the blade height in D1. Slots located further away from the endwall, such as those at 15% and 25% of the blade height in D2 and D3, have little effect on static pressure distribution on the endwall.

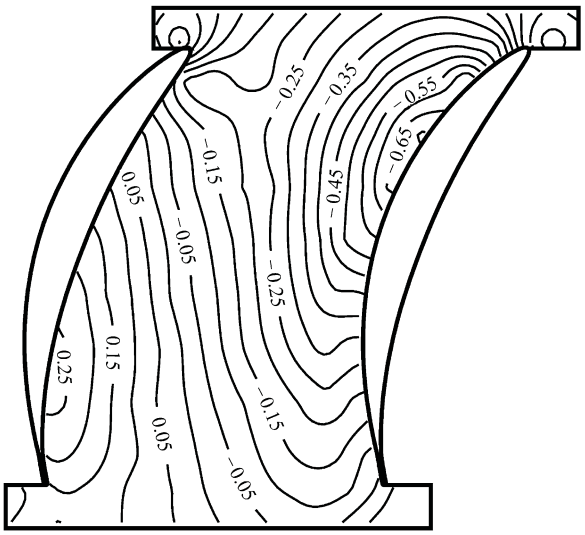

(a) D0

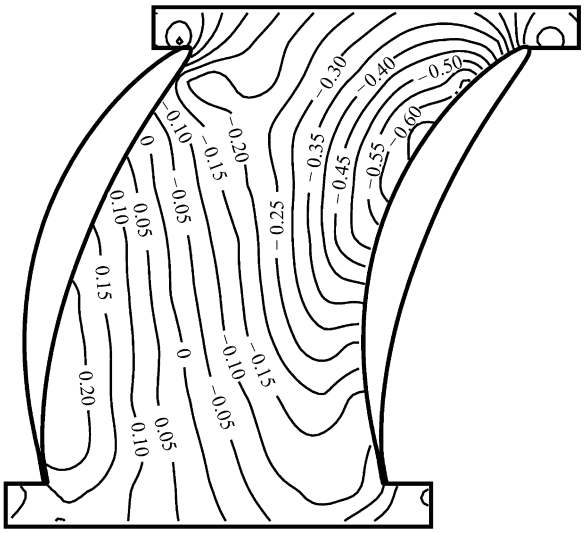

(b) D1

Fig.3 Contours of static pressure coefficients on cascade endwall.

Fig.4 shows ink-trace flow visualization on the blade suction surfaces. In all cases, the passage vortex separation line, in Fig.4 for D0 case, can be seen originating at approximately 43% chord from the leading edge at the endwall. For D0, the separation line stretches diagonally and extends along the span to about 40% of blade height from the endwall at the trailing edge. Table 1 lists the heights of separation lines (H_{sl}) for all cases. The height of separation line, which is related to the losses, reduces significantly because of air injection through the slots. From Table 1, it is found that the flow behavior near the midspan improves for D3, D5, D6, and D7 agreeing with the distribution of energy losses at the cascade exit. It might be concluded that air injection through slots, especially, the slot located at 25% of the blade height decreases separation zone. This is perhaps attributed to the air injection at this blade height that, with high momentum, prevents the low-energy fluid from accumulating at the midspan.

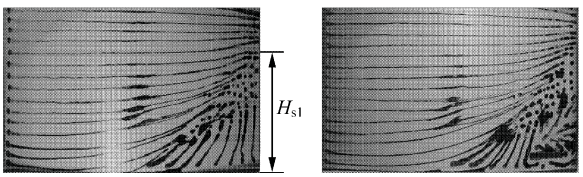

(a) D0 (b) D1

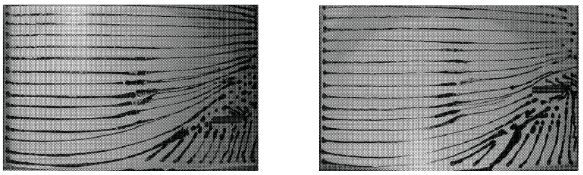

(c) D2 (d) D3

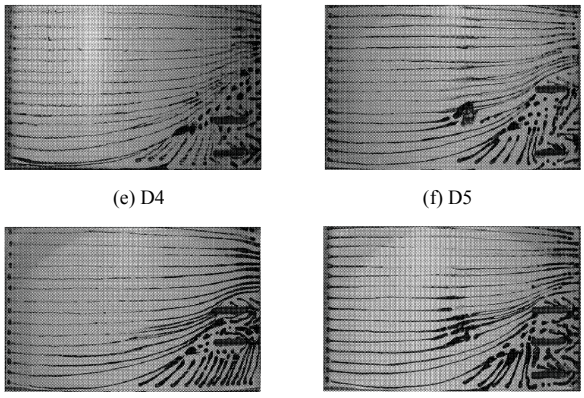

(e) D4 (f) D5

(g) D6 (h) D7

Fig.4 Ink-trace flow visualization on blade suction surfaces.

Table 1 Heights of separation lines

Case	$\frac{H_{sl}}{H}$ /%
D0	40.00
D1	40.00
D2	34.40
D3	32.50
D4	35.00
D5	32.80
D6	31.25
D7	31.25

To show the influences of air injection on losses, Fig.5 illustrates contours of energy loss coefficient ξ with and without air injection. Here, the energy loss coefficient is defined as

$$\bar{\xi} = \frac{(p_s / p^*)^{(k-1)/k} - (p_s / p_1^*)^{(k-1)/k}}{1-(p_s / p_1^*)^{(k-1)/k}} \tag{2}$$

where p^* is local total pressure. For ideal air, $k = 1.4$.

For D0, the boundary of the loss region near the pressure side extends pitch-wise to 63.8% pitch. It could be expected that there is a separation leading to a

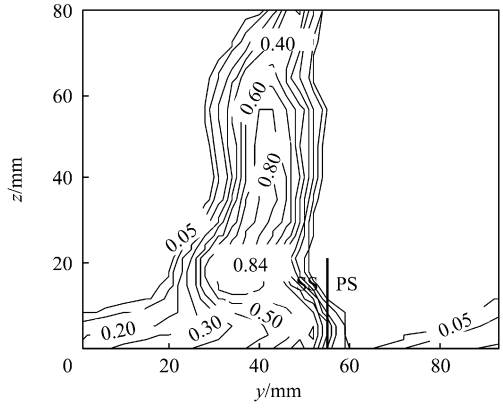

(a) D0

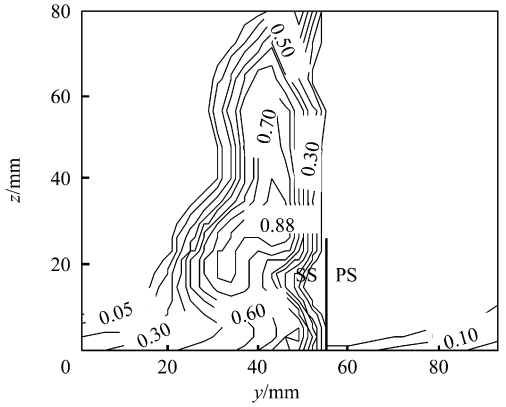

(b) D1

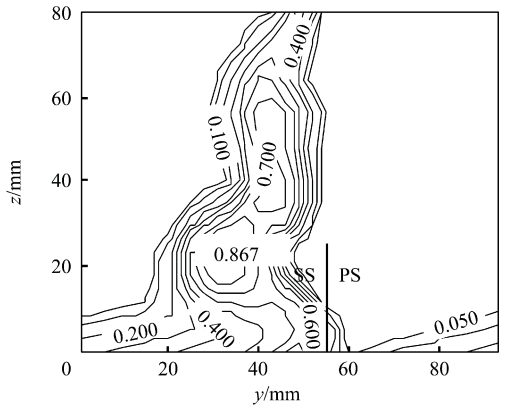

(c) D2

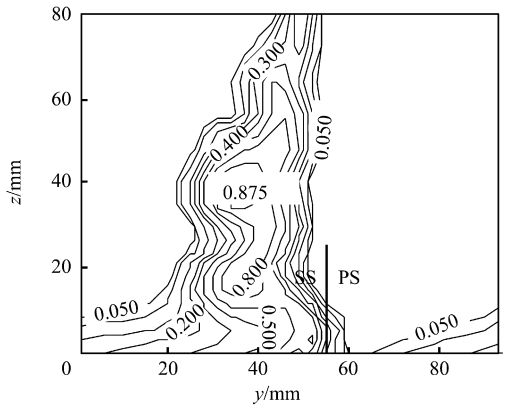

(d) D3

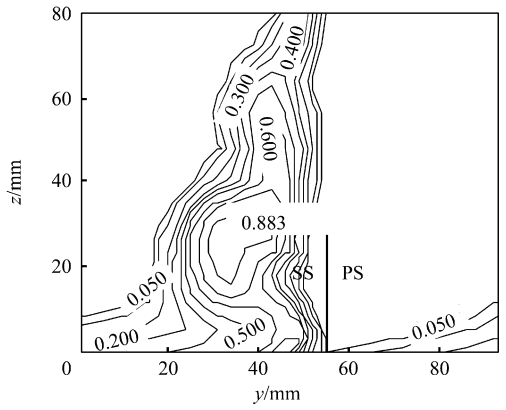

(e) D4

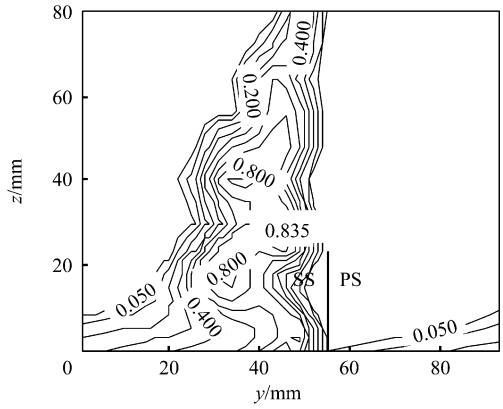

(f) D5

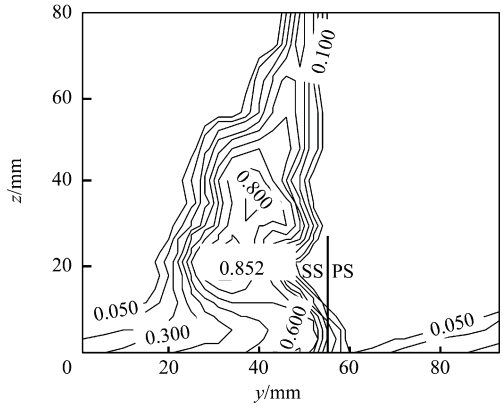

(g) D6

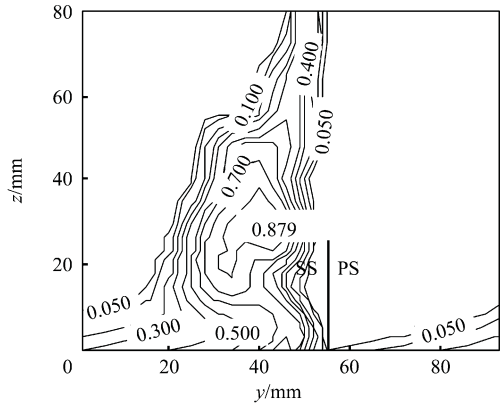

(h) D7

Fig.5 Contours of energy loss coefficient at outlet.

large loss near the midspan. For D1, the region of high energy losses is almost the same as that in the case of baseline. Loss near the endwall decreases, and the boundary of the loss region near the pressure side extends to 58.5% pitch, which is the same with D4, D5, and D7. This might be ascribed to the air injection at 5% span, which improves flow and decreases losses near the endwall. The measured maximum loss core represented by the local value for each configuration is concentrated on within 18.75% span of the endwall and approximately 14% pitch from the pressure side. For D2, losses increase near the maximum loss core at 12.5% span and decrease further away from it. Similar effects can be seen for D3. The maximum loss core is at around 25% span. This can be blamed for the mixing loss by the jet through the slot located at 25% span. Loss decreases dramatically near midspan. For D4 with slot at 5% and 15% span, the maximum loss core position is similar to that of D1, but the loss region near it increases greatly compared to that of D0. For D5, three high loss cores can be seen from the figure. The core on the top is almost identical with that of D3, and the other two cores look like those of D1. For D6 and D7, losses near the midspan decrease significantly. Conclusion can be drawn from the above observation that air injection increases losses near the slots, but then decreases them further from the slots in contrast to the baseline. In case of the slot located at 5% span, losses near the slot increase greatly, especially, in a multislot configuration, such as D4 and D7. Losses near the midspan will decrease to the most if the slot is located at 25% span (such as the cases of D3, D5, D6, and D7).

Fig.6 shows the distribution of the secondary flow vectors and streamlines in the eight cases. The results show the effects of air injection on the secondary flow, for example, the spanwise location of the passage vortex core, which presents the concentrated region in all cases. The streamlines of secondary flow stemming from the endwall near the suction side (marked by dark line) for D0 is approximately 2.66% pitch from the suction side. For D1-D3, the distances are about 7.4%, 3.2%, and 3% pitch respectively. For multislot configurations D4-D7, the distances are about 7.4%, 5.85%, 3.7%, and 6.9% pitch from the suction side. In comparison with the baseline, air injection tends to push the passage vortex away from the suction side. From the above observation, it might be concluded that air injection from the slot at 5% span has visible effects on the reduction in the width of the passage vortex, while injection from the slot at 15% and 25% span has not.

The spanwise variations of the pitch-averaged energy loss coefficient are plotted in Fig.7. The baseline configuration shows a higher loss across the blade covering up to approximately 42% span away from the endwall. High losses are caused by the severe flow separation because of the large camber angles. In all configurations, losses are more or less identical from the endwall at 0%-10% span. Air injection causes an increased loss near the slot in comparison with the case of baseline configuration. The increased loss is a mixing loss caused by fluids mixing around the slot near the suction side. Near the midspan, losses decrease at approximately 30%-50% span in all cases. In one slot configurations, remarkable decrease in losses only occur in D3 while smaller one in others. In all multislot configurations, significant decreases in losses can be seen near the midspan. Of them, the slot 3 is found to have great effects on reducing losses near midspan, and the maximum reduction in losses near midspan could be acquired in D6 and D7.

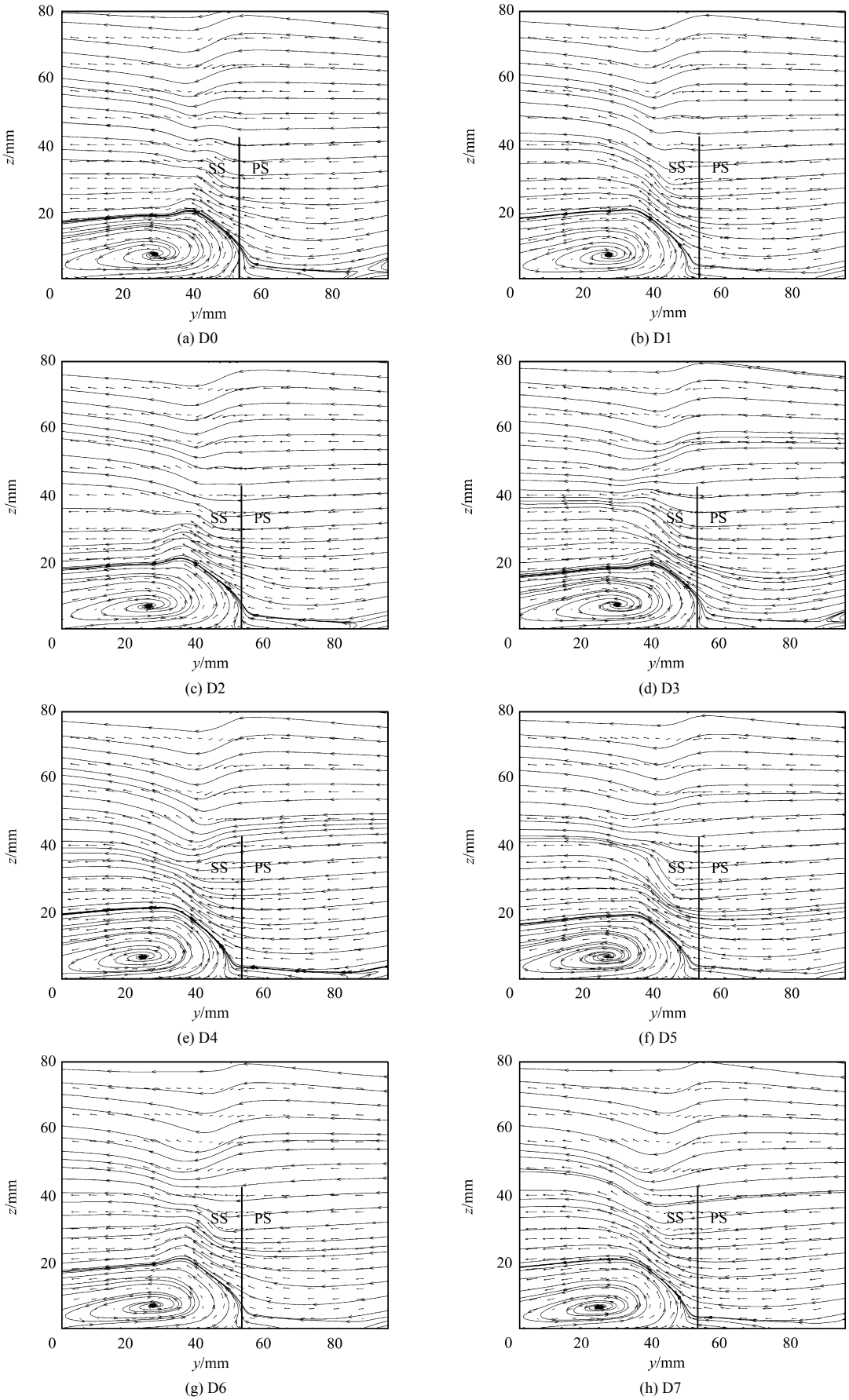

Fig.6 Distribution of secondary flow vectors and streamlines at outlet.

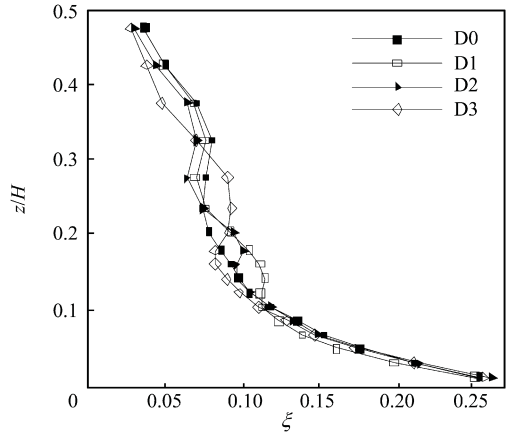

(a) One slot configurations

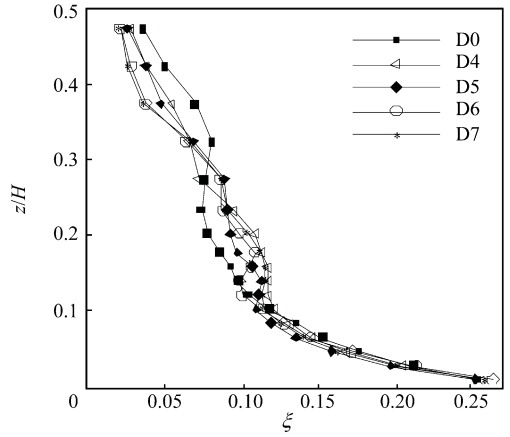

(b) Multislot configurations

Fig.7 Spanwise distribution of mass-averaged energy loss coefficients.

In order to clarify the overall improvements of aerodynamic performances by air injection, Table 2 lists the increments of energy loss coefficient, which is defined as

$$\Delta\xi = \left(1 - \frac{\xi_{\mathrm{m}}}{\xi_{\mathrm{m0}}}\right) \times 100\% \tag{3}$$

where ξ_{m0} is the energy loss coefficient of D0 and ξ_{m} the energy loss coefficient with air injection slot(s).

Table 2 Increments of energy loss coefficient

Case	$\Delta\xi$/%
D0	0
D1	0.48
D2	2.92
D3	4.75
D4	–1.96
D5	3.69
D6	5.52
D7	4.53

The losses in D1 are close to those in D0, while losses in others decrease significantly except for in D4, whose losses increase instead. From Fig.7, it is visible that losses increase in presence of slots because of the mixing. Air injection restrains the low-energy fluid moving towards the midspan, meanwhile, high-speed fluid injected from the pressure side drives the low-energy fluid in the midspan downstream. The decrease in losses near the midspan is more than the increase of the mixing loss near the slot caused by air injection. The maximum relative reduction of energy loss coefficient is 5.5 % for D6. The optimal slot location seems to be at 25% of blade span, since all configurations with this slot location (D3, D5, D6, and D7) produce relatively more significant effects on reducing losses.

The spanwise variations of the pitch-averaged diffusion factor are plotted in Fig.8 for one slot configurations (top) and multislot configurations (bottom), each including the baseline. The mass-averaged diffusion factor (DF) is defined as

$$\mathrm{DF} = 1 - \frac{V_2}{V_1} + \frac{V_{\mathrm{t1}} - V_{\mathrm{t2}}}{2\tau V_1} \tag{4}$$

where V_1 and V_2 are the velocities at the blade inlet and outlet, V_{t1} and V_{t2} the tangential velocities at the same

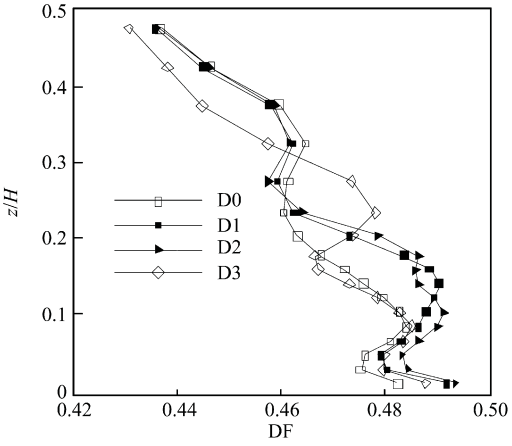

(a) One slot configurations

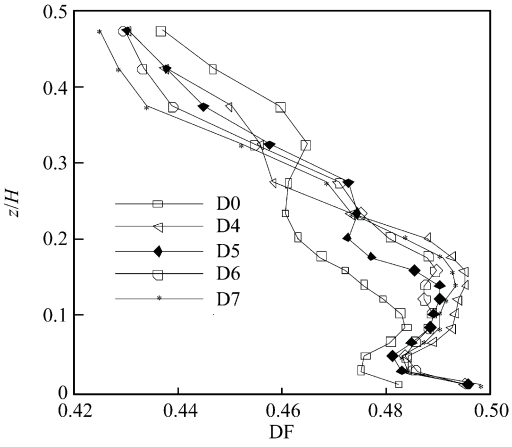

(b) Multislot configurations

Fig.8 Spanwise distribution of diffusion factor.

places as V_1 and V_2, and τ the solidity defined as the chord divided by the pitch.

In all cases, DF reaches the maximum at 8%-16% span near the endwall. For D1 and D2, their DFs are nearly identical at 25%-50% span in contrast to D0. A large increase in DF can be seen from the endwall to 25% span. The increase in DF peaks close to the slot locations indicates a blade loading increase caused by air injection. For D3, its DF increases from 18% to 30% span, then decreases further up to 50% span. Similar distribution can be seen from Fig.7, because greater blade loading is associated with increased losses. For multislot configurations, DF increases from the endwall to approximately 30% span in all cases, and then decreases from 30% to 50% span.

4. Conclusions

An experimental proof-of-concept test was conducted to demonstrate reduction of losses in highly loaded compressor linear cascades via air injection. Conclusions are made as follows:

(1) Air injection at 5% span has an effect on static pressure at the endwall. In other cases, static pressure changes less significantly than the baseline configuration.

(2) Air injection through the slot(s) from pressure side to suction side with high velocity prevents low-energy fluid from accumulating at midspan thus decreasing the flow separation area near the midspan. The size of the spanwise flow separation region reduces significantly because of air injection through the slot(s), especially when the slot is located at 25% span.

(3) Energizing the low-energy fluid near the suction surface, air injection produces the positive effects to decrease losses caused by the accumulated low-energy fluid near the midspan and the negative effects to increase mixing losses near the slot.

In the end, because the effectiveness of the presented air injection method is more likely dependent on specific case, further efforts should be devoted to develop more effective configurations with high aerodynamic performances under off-design conditions (such as different incidences).

References

[1] Gad-el-Hak M. Modern developments in flow control. Applied Mechanics Reviews 1996; 49: 365-379.
[2] Greenblatt D, Wygnanski I J. The control of flow separation by periodic excitation. Progress in Aerospace Sciences 2000; 36(7): 487-545.
[3] Bons J P, Sondergaard R, Rivir R B. Turbine separation control using pulsed vortex generator jets. Journal of Turbomachinery 2001; 123(2): 198-206.
[4] Volino R J. Separation control on low-pressure turbine airfoils using synthetic vortex generator jets. Journal of Turbomachinery 2003; 125(4): 765-777.
[5] Parekh D E, Glezer A, Allen M, et al. AVIA: adaptive virtual aerosurface. AIAA-2000-2474, 2000.
[6] Honohan A M, Amitay M, Glezer A. Aerodynamic control using synthetic jets. AIAA-2000-2401, 2000.
[7] Zheng X Q, Zhou X B, Zhou S. Investigation on a type of flow control to weaken unsteady separated flows by unsteady excitation in axial flow compressors. Journal of Turbomachinery 2005; 127(3): 489-496.
[8] Song Y P, Chen H L, Chen F, et al. Effects of air injection on performance of highly-loaded compressor cascades. ASME 2007-GT-27062, 2007.
[9] Zhao G J. Investigation of boundary condition and secondary flow control in curved-swept compressor cascade. PhD thesis, Harbin Institute of Technology, 2005. [in Chinese]

Biographies:

Feng Dongmin Born in 1979, he received B.S. degree from Harbin Engineering University in 2003 and M.S. degree from Harbin Institute of Technology in 2005, and now study as a Ph.D. candidate in School of Energy Science and Engineering, Harbin Institute of Technology. His main research interest is in the area of turbomachinery aerodynamics.
E-mail: fengdongmin@163.com

Chen Fu Born in 1970, he is a professor in School of Energy Science and Engineering, Harbin Institute of Technology. His main research interest is in the area of turbomachinery aerodynamics.
E-mail : chenfu@hit.edu.cn